Minor Complexes at Work: Light-Harvesting by Carotenoids in the Photosystem II Antenna Complexes CP24 and CP26

Alessandro Marin,[†] Francesca Passarini,[‡] Ivo H. M. van Stokkum,[†] Rienk van Grondelle,[†] and Roberta Croce[‡*]
[†]Faculty of Sciences, Vrije Universiteit Amsterdam, De Boelelaan, Amsterdam, The Netherlands; and [‡]Department of Biophysical Chemistry, Groningen Biomolecular Sciences and Biotechnology Institute, University of Groningen, Groningen, The Netherlands

ABSTRACT Plant photosynthesis relies on the capacity of chlorophylls and carotenoids to absorb light. One of the roles of carotenoids is to harvest green-blue light and transfer the excitation energy to the chlorophylls. The corresponding dynamics were investigated here for the first time, to our knowledge, in the CP26 and CP24 minor antenna complexes. The results for the two complexes differ substantially. In CP26 fast transfer (80 fs) occurs from the carotenoid S_2 state to chlorophylls *a* absorbing at 675 and 678 nm, whereas transfer from the hot S_1 state to the lowest energy chlorophylls is observed in <1 ps. In CP24, energy transfer from the S_2 state leads in 80 fs to the population of chlorophylls *b* and high-energy chlorophylls *a* absorbing at 670 nm, whereas the low-energy chlorophylls *a* are populated only in several picoseconds. The results suggest that CP26 has a structural and functional organization similar to that of LHCII, whereas CP24 differs substantially from the other Lhc complexes, especially regarding the lutein L1 binding domain. No energy transfer from the carotenoid S_1 state to chlorophylls was observed in either complex, suggesting that this state is energetically below the chlorophyll Qy state and therefore may play a role in the quenching of chlorophyll excitations.

INTRODUCTION

Plants are able to produce organic compounds consuming carbon dioxide, water, and energy from light. Two large pigment-protein complexes in the thylakoid membrane of the chloroplast, Photosystems I and II, perform the first stages of the solar energy storage reactions. Each photosystem is composed of two elements: the reaction center, where the actual energy conversion takes place, and the antenna complexes, whose role it is to absorb sunlight and funnel the electronic excitation to the reaction centers. Photosystem II consists of a core complex containing 36 chlorophylls (Chls) and several carotenoids (Cars) (1). It is surrounded by four peripheral antenna complexes: the major antenna light-harvesting complex II (LHCII), present as a trimer in the membrane, and the three minor antenna complexes CP24, CP26, and CP29 (2,3). Each one includes a collection of pigments, Chls and Cars, held in place by coordination to specific residues or molecules. Hence, funneling of energy from antennas to reaction centers is effectively carried out by means of excitation energy transfer (EET) between (groups of) pigments (for details see Croce and Amerongen (4)). However, these complexes also have a second role: in high light, when the maximal rate of the converting energy process is not sufficient to process the number of harvested photons, they are able to dissipate the excess absorbed energy and avoid damage in a process called non-photochemical quenching (NPQ) (5–7).

The crystal structure of trimeric LHCII (8,9) shows the presence and positions, per monomeric unit, of 14 Chls – six Chls *b* and eight Chls *a* – and four Cars – two Luteins (Luts) in the L1 and L2 sites, one Neoxanthin (Neo) in the N1 site, and one Violaxanthin/Zeaxanthin (Vio/Zea) in the V1 site (10–13). Furthermore, very recently the structure of CP29 has become available, showing a pigment organization very similar to that of LHCII, although the occupancy of several binding sites is different (14). Although the minor antennas CP24 and CP26 are supposed to be homologous to the monomeric subunit of LHCII, so far their structures are unknown. The pigment organization in antenna complexes has been intensely investigated using the in vitro reconstitution approach (15,16), by reconstituting the complexes in the presence of different pigments (17–19), and by analyzing a series of single point mutants affecting the pigment binding (20–22). These studies have shown that the minor antenna complexes contain two (CP24) or three (CP29 and CP26) Car binding sites. Site L1 hosts Lut in all complexes, whereas site L2 accommodates Lut in CP26, and Vio in CP29 and CP24. Neo is bound to site N1 in CP26 and CP29 (23) and is absent in CP24 (22).

Spectral properties of Cars have been extensively studied in solution where interactions with other pigments are absent (for a review, see Polívka (24)). However, fundamental photosynthetic processes such as light-harvesting and photoprotection (triplet quenching and singlet quenching) are based on Car-Chl interactions, which are induced by the presence of the protein. Car-Chl interaction studies in antenna complexes of higher plant were performed only on LHCII and CP29, either using femtosecond spectroscopy (25–30), triplet-minus-singlet spectroscopy (31–37), or steady-state spectroscopy (38,39). It was shown that, out of the four Cars associated with LHCII, three are active in EET (12) and two in triplet quenching (32). In vitro analysis of Lhc complexes has also suggested that one of these

Submitted December 16, 2010, and accepted for publication April 12, 2011.

*Correspondence: r.croce@vu.nl

Editor: Leonid S. Brown.

0006-3495/11/06/2829/10 $2.00

doi: 10.1016/j.bpj.2011.04.029

xanthophylls is active in singlet quenching. Three different proposals have been put forward: i), Lut in the L1 site of LHCII is responsible for quenching, via interaction with Chls 610/611/612 (40); ii), the quenchers are Car-Chl states, since electronic interactions between Car S_1 and Chls were shown to scale with the amount of NPQ (41); and iii), the quencher is Zea located in the L2 site of the minor antenna complexes, via the formation of a radical cation (42). More recently it has been shown that a radical cation can be formed in CP29 and CP24 also on the Lut in the L2 site (43). As this is never the case for LHCII and CP26, variations in the Car-Chl interactions within the different complexes were suggested. This should not be the case for the L1 site, because it was shown by steady-state spectroscopy that the domain composed of Lut L1 and Chls 611/612 is completely conserved in LHCII, CP29, and CP26, whereas it partially differs only in CP24 (38), suggesting that if Lut acts as a quencher in LHCII it should have the same effect at least in CP26 and CP29.

The excitation energy transfer studies on LHCII and CP29 show that in these two complexes most of the energy is transferred from the S_2 state of the Cars to Chls. In LHCII, Lut in the L1 site transfers to low-energy Chls *a* (27,28,33) in $<$100 fs, whereas Neo in the N1 site of LHCII was shown to transfer only to Chls *b* on a similar time scale (27,28). Different results were obtained in the case of Lut in the L2 site of LHCII and for Neo in the N1 site of CP29: in both cases Gradinaru et al. (27) reported only transfer to Chls *a*, whereas Croce et al. (28,29) reported transfer also to Chls *b*. All these reports indicate 15–20% of Car to Chl EET from the vibrationally hot S_1 state of at least one xanthophyll molecule.

The rather fast rate of EET from the Car hot S_1 state to the Chl Q_y state suggests an electronic coupling between the two states. In case the two states become quantum-mechanically mixed, the coupling would be large enough to influence the excited-state lifetime of Chls. Relatively subtle changes in the coupling strength may produce a strong quencher, which was proposed to be at the basis of NPQ (44). Recently, Bode et al. (41) showed a strong correlation between the intensity of the Car-Chl interactions in vivo and the levels of NPQ, supporting the previous hypothesis.

This work integrates our previous study (45) describing the EET dynamics in CP26 and CP24 upon excitation of the Chls in the Qy region. CP26 was found to have Chl *b* to Chl *a* EET dynamics similar to those of LHCII, although slightly faster (0.21 and 1.5 ps vs. 0.13, 0.6 and ~3.3 ps). The intermediate state region (660–670 nm) is reduced in amplitude as compared to LHCII, but retains both fast (0.32 ps) and slow (3.5–15 ps) dynamics. In CP24 two bands at 640 and 653–654 nm absorb in the Chl *b* region; 86% of Chl *b* transfer occurs in 0.61 ps to two Chls *a* bands at 670 and 675 nm. The 670 nm band, in particular, is strongly enhanced as compared to the other Lhc complexes; it interacts with Chls *b* and completely decays in 3–5 ps to the lowest energy states. This band, attributed to Chl *a*602 and/or *a*603, mediates energy migration to the lowest energy states (Chls 611–612).

In this work, we investigate Car to Chl energy transfer in CP26 and CP24. Femtosecond transient absorption spectroscopy is employed to explore the Cars excited state dynamics and the energy exchange between pigments.

MATERIALS AND METHODS

Sample preparation

The mature DNA sequences coding for CP24 (AT1G15820) and CP26 (AT4G10340) were amplified from an *Arabidopsis thaliana* cDNA library by PCR using specific primers. The amplified sequences were then cloned in a modified pET-28a(+) vector carrying a minimum polylinker and overexpressed in the Rosetta2(DE3) strain of *Escherichia coli*. The apoproteins were purified as inclusion bodies and the pigment-protein complexes were reconstituted as in (10) using a mix of purified pigments extracted from spinach with a Chls *a*/*b* ratio of 2.9 and Chls/Cars ratio of 2.7. The purification of the antenna complexes from unfolded proteins and free pigments was performed as described in Passarini et al. (22).

77 K steady-state absorption spectra and pigment content analysis

The 77 K absorption spectra were recorded using a Cary 4000 spectrophotometer (Varian, Palo Alto, CA) at a Chl concentration of ~6 μg/ml in 10 mM HEPES pH 7.5, 0.03% β-DDM, and 70% v/v glycerol. The pigment complement was determined as in (19).

Transient absorption experiments

A description of the experimental setup, data analysis, and reconstitution procedure was reported elsewhere (45). Briefly, experiments were carried out in a 1 kHz pump-probe setup with pump tuned at 506 or 490 nm and 5–7 nJ of excitation intensity. A liquid nitrogen cryostat (Oxford DN-900, Oxford, UK) was used for 77 K experiments. The preparations were contained in a 1 mm cuvette with OD ~0.4/mm. The recorded time-resolved data cover a 425–710 nm spectral range with 1.2 nm resolution, and the maximum time delay between pump and probe was 3.4 and 7.6 ns for CP26 and CP24, respectively. The recorded data were analyzed with global and target analysis (46). Fig. S1 and Fig. S2 in the Supporting Material show the fit of selected traces after fitting. In global analysis an unbranched, sequential model of *n* compartments (i.e., $1 \rightarrow 2 \rightarrow \ldots \rightarrow n$) is used. Each compartment is described by an Evolution Associated Difference Spectrum (EADS) that exponentially evolves into the next with its associated lifetime (i.e., see Fig. 2: the first EADS (EADS1) is present after excitation and decays in 78 fs, EADS2 rises in 78 fs and decays in 1.2 ps, and so on). The last component is given an infinite decay, meaning that its decay is too slow to be determined with the experimental time range. The estimated EADS represent a mixture of excited states and, together with the lifetimes, describe the spectral evolution of the pump-probe data.

Target analysis

To estimate the spectra of pure excited states, target analysis was performed on the pump-probe data using the compartmental schemes (see Fig. 7, *A* and *B* (vide infra)). Spectral assumptions on the species-associated difference spectra (SADS) were necessary to resolve the spectra (see Figs. 5 and 6): 1), the spectra for Car S_1 and hot S_1 state have zero contribution in the

Chl Qy region (above 650 and 640 nm, respectively) and have equal spectra in the bleach (below 506/510 nm, in CP26/CP24). Without the first constraint the SADS become unrealistic in the Chl Qy region due to compensatory effects. The equality of the bleach is an approximation of the Car S_1 spectra found in the global analysis; 2), the spectrum of Chl *b* compartments was zeroed in the Chl *a* Qy region (above 662 nm); and 3), the spectra of the Chls *a* compartments (i.e., Chl a1, Chl a2, and Chl a3) have equal Chl ESA up to 635/659 nm in CP26/CP24; 4), the Chl b compartment has the same Chl ESA (in the 507–632/511–641 nm range in CP26/CP24) as Chl a2 and a3. All assumptions were necessary to prevent mixing of different Car-Chl or Chl *b*-Chl *a* dynamics leading to bad estimations of the kinetic rates.

RESULTS

Absorption spectra and carotenoid excitation

The absorption spectra of CP24 and CP26 at 77 K are reported in Fig. 1 *A*. The second derivative of the spectrum of CP26 in the Car absorption region (Fig. 1 *B*) shows a single peak at 493 nm. This peak is likely to contain contributions of the two Luts located in the L1 and L2 sites, whereas Neo in the N1 site is probably responsible for the shoulder around 488 nm. At room temperature (RT) these Cars show absorption maxima at 491, 494, and 488 nm, respectively (21,23). The fact that the absorption spectra of the different xanthophylls associated with CP26 nearly coincide hinders selective excitation of the different species. To study the Car to Chl energy transfer, we have thus chosen to excite the sample at 506 nm, a region dominated by the Cars absorption where the direct Chls excitation is strongly reduced (17,29). In the case of CP24, the second derivative of the absorption spectrum shows two contributions at 498 and 503–504 nm, which should correspond to the absorption maxima at 77 K of Lut-L1 and Vio-L2 (22). The spectra of the xanthophylls largely overlap, making selective excitation of the individual xanthophylls practically impossible.

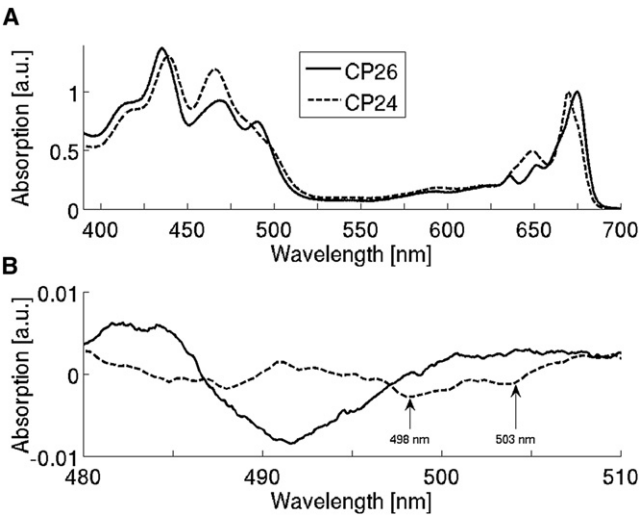

FIGURE 1 (*A*) OD spectra for CP26 (*solid*) and CP24 (*dashed*). (*B*) Second derivative of the OD spectra in the 480–510 nm range.

In the attempt to excite the two xanthophylls in different ratio, we present two measurements on CP24 with excitation at 506 and 490 nm.

CP26 excited at 506 nm

The global analysis applied to the pump-probe data is shown in Fig. 2. The first component is dominated by the presence of excited Car S_2 state(s), as most probably only a small fraction of Chls is directly excited. The spectrum is composed of a negative band (bleach/stimulated emission (SE)) at 500 nm, a shoulder at 470 nm, and pronounced negative features at 533, 543, 589 nm. A positive band (due to excited state absorption (ESA)) above 640 nm is present with superimposed Chl bleaching bands at 636, 654, and 675 nm. The first evolution shows internal conversion to the vibrationally hot S_1 states plus EET to the Chls in 78 fs. A broad ESA typical of hot Car S_1 states (47–50) is formed in the 505–630 nm part of the spectrum. The Car bleach/SE features a decay in amplitude of 77% and a blue shift to 495 nm of ~5 nm; this shift and part of the decay derive from the absence, in EADS2 compared to EADS1, of the SE part of the ΔOD signal originating from the Car S_2 states. In the Qy the Chl *b* bleaching at 636 nm decreases as compared to EADS1, and energy transfer is directed to the Chls *a*. The Chl *a* increase indicates transfer to two Chl *a* populations at 674–675 and 678–679 nm. This is better visible in the first Decay Associated Difference Spectum (DADS) in Fig. S3, which shows the decayed or gained signal in the first 78 fs evolution.

EADS3 takes the place of EADS2 in 1.2 ps. In the 560–625 nm part of the spectrum the narrowing of the Car ESA denotes vibrational relaxation of the Car hot S_1 to the Car S_1 states. The Car bleach shows a reduction of 57% in area. Transfer from Chls *b* to Chls *a* and a red shift of the Chl *a* bleach/SE from 676.6 to 677.8 nm is observed in the Qy region.

The 15.0 ps lifetime is mainly determined by the evolution in the Car range, showing the decay of the Car ESA below 630 nm. In this transition the Qy bleach shifts to 679.0 nm and EADS4 becomes positive below 671 nm, denoting the decay of blue Chls *a* (cf. the DADS in Fig. S3).

EADS4 decays with 3.9 ns, and is attributed to the Chl *a* decay. The last component is necessary to fit the species appearing at late delay times in the ~470–550 nm region. This EADS has the characteristic shape of the long-lived carotenoid triplet (CarT). The peak at 509.2 nm and a bleach/SE at ~496 nm can be attributed to the Lut triplet (32). The hint of a shoulder at 520 nm suggests the presence of a second triplet form.

CP24 excited at 506 nm

For CP24 the global analysis of the 506 nm excitation data is shown in Fig. 3. The Car bleaching in the initial EADS

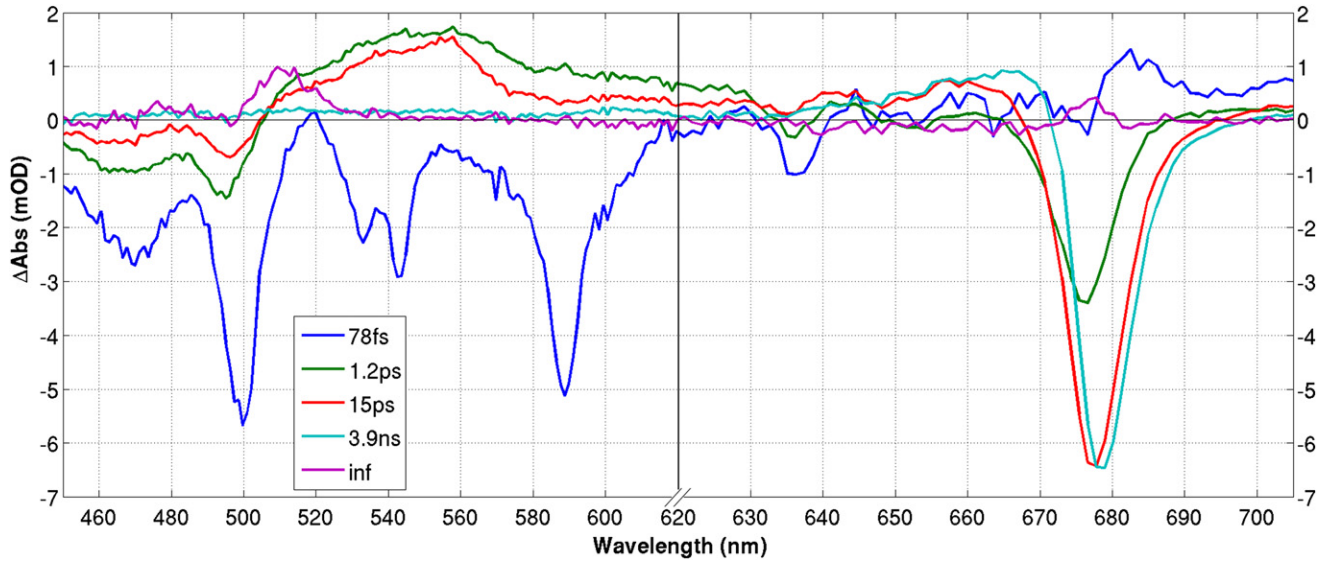

FIGURE 2 Global analysis results (EADS and connecting lifetimes) of the pump-probe measurements on CP26 at 77 K after 506 nm excitation. Notice the change in scaling of the *x* axis at 620 nm.

peaks at 504 nm, and peaks are present at 540, 549, and 598 nm. A small bleach/SE is present in the Chl *b* Qy region superimposed to an ESA covering the Chl Qy region, together with a bleached Chl *a* band at 671 nm. Formation of Car hot S_1 parallels the population of Chls *b* (655 nm) and Chls *a* (671 nm) by the decay of Car S_2 states in 80 fs. In the following 0.52 ps transition Car S_1 states appear, the Chl *b* band decays almost completely and the Chls *a* display a broad bleach/SE peaking at 672.4 nm, composed of two bands at ~671 and 677 nm. The third 3.3 ps lifetime describes the equilibration of the Chls *a* at 670 nm with the low-energy Chl *a* forms.

The 20.5 ps transition represents the decay of the residual Car S_1 ESA, although a better estimate is the 14.7 ps Car S_1 lifetime found in the target analysis (vide infra). Indeed, the same component (again 14.7 ps) is observed also by global analysis when only the 490–610 nm region of the spectrum is analyzed (Fig. S4). The 20.5 ps found is likely the result of the presence of the 3.3 ps transition ascribed to the Chls, which is needed for the description of the Qy region and yields a slow fourth lifetime in the order of 20 ps in the Car region.

The fifth 2.9 ns component shows the Chl *a* excited state decay. The last infinite component is needed to fit the CarT

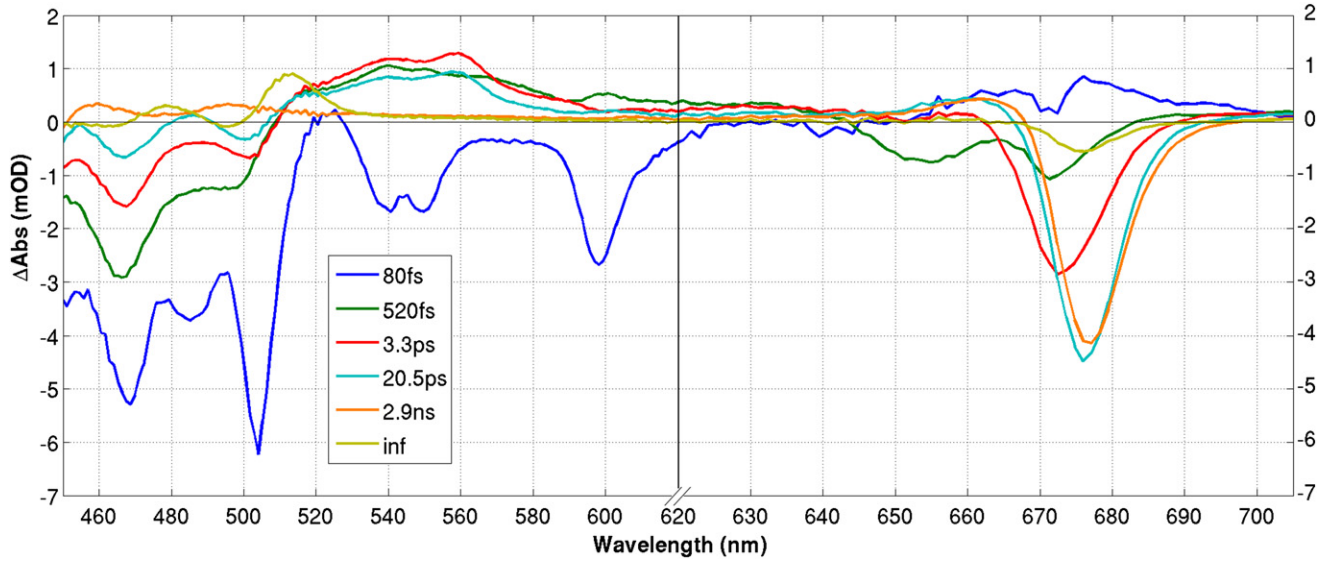

FIGURE 3 Global analysis results (EADS and connecting lifetimes) of the pump-probe measurements on CP24 at 77 K after 506 nm excitation. Notice the change in scaling of the *x* axis at 620 nm.

rise: the spectrum has maxima and minima at 513/478 and 496/464 nm, respectively.

CP24 excited at 490 nm

The global fit for CP24 excited at 490 nm is shown in Fig. 4. The resulting analysis resembles the one in Fig. 3; very similar lifetimes describe the Car internal conversion processes (110 fs, 24.0 ps), Car vibrational relaxation and Chl *b* decay (540 fs) and decay of the Chl *a* at 670 nm (3.6 ps). In the Qy region only a positive ESA signal is visible with no clear Chl *b* or *a* bleaching. Except for a reduction of the S_2 to Chl *a* pathway after 490 nm excitation (compare the relative amplitudes of Chls *b* with Chls *a* in the second EADS for the two excitations), both CP24 datasets show analogous EET pathways from Car S_2 to Chl *b* and to Chls *a* (mostly at 670 nm). This confirms that the different excitations are only partially selective, i.e., both Lut-L1 and Vio-L2 are excited at 506 and 490 nm albeit in different ratios.

Target analysis of CP26

Excitation of CP26 and CP24 in the Car region yields complex kinetics, which result from several Car and Chl independent processes taking place concomitantly. Target analysis was applied to the data of both complexes upon excitation at 506 nm to disentangle contributions of different pigments and to obtain rate constants of different processes. The proposed photophysical model (see Fig. 7, *A* and *B*) is shown in the form of compartmental schemes. For CP26 (see Fig. 7 *A*) eight species are needed to describe the data, where several spectral constraints enable resolving the different species (see Materials and Methods). All spectral evolutions in the Qy region can be assigned to four Chl compartments denoted with the tags Chl b, Chl a1, Chl a2, and Chl a3. Four SADS associated with the Car S_2, hot S_1, S_1, and CarT states were resolved; see Fig. 7 *A* for the estimated rate constants. Branchings from Car S_2, hot S_1, and S_1 states to Chl *b*, Chl a1, and Chl a2 are needed for an optimal fit and are discussed later (vide infra).

The SADS obtained from the target analysis are shown in Fig. 5. A lifetime of 0.89 ps was found for the Car hot S_1 relaxation (the sum of the two transitions described by the k4 and k5 rates, see Fig. 7 *A*), and optimization of the Car S_1 decay rate led to a 15.0 ps lifetime as in the global analysis. The Car S_2 compartment decays to Car hot S_1 (30%), Chl a1 (60%). The remaining 10% transfer occurs to Chl *b* and is needed for an optimal fit, although in Fig. 2 it is difficult to clearly resolve EET to the Chls *b* due to the presence of an initial Chl *b* bleaching. The three Chl *a* spectra show a progressive shift to longer wavelengths as a result of Chl intraband equilibration. Branching from the Car hot S_1 state to Chl a2 leads to ~15% transfer of the hot Car excitation to the Chl a2 compartment. The CarT SADS is substantially identical to the last EADS in the Car region (Fig. 2).

Target analysis of CP24

Target analysis was applied to the CP24 506 nm data set of Fig. 3. The compartmental scheme used (see Fig. 7 *B*) is the same as the one in Fig. 7 *A*. The 80 fs lifetime of the Car S_2 compartment (Fig. 6) confirms the one in the global analysis (Fig. 3), and therefore the SADS nearly coincides with EADS1. From the S_2 state, 30% and 25% of the energy was transferred to Chls *a* and Chls *b*, respectively, whereas the other 30% ended up in the hot S_1 state. A 0.59 ps lifetime

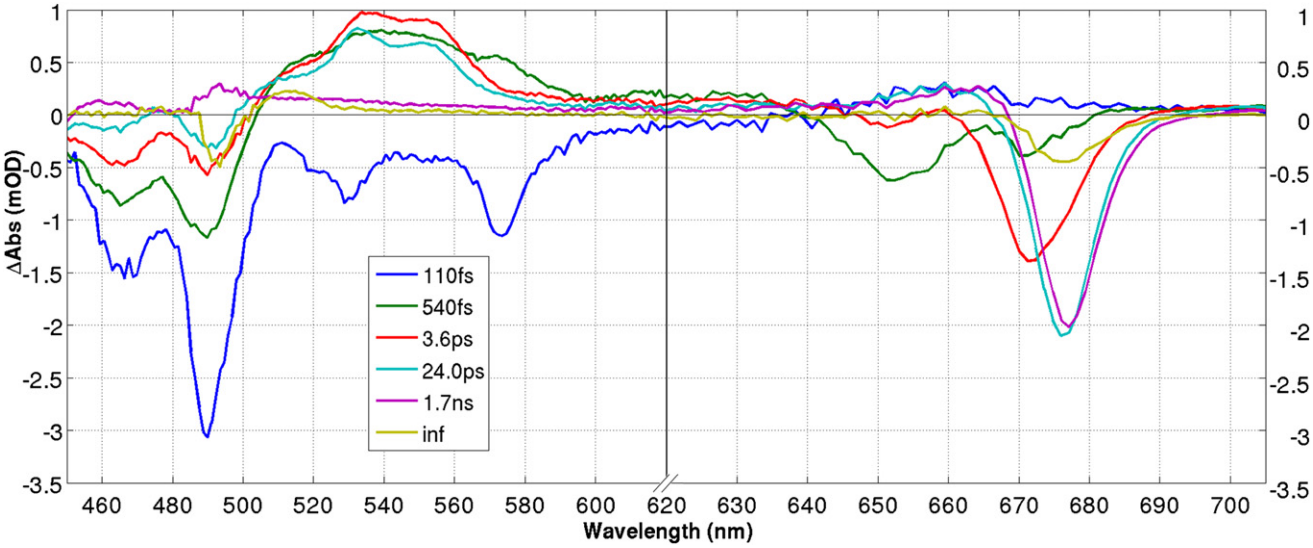

FIGURE 4 Global analysis results (EADS and connecting lifetimes) of the pump-probe measurements on CP24 at 77 K after 490 nm excitation. Notice the change in scaling of the *x* axis at 620 nm.

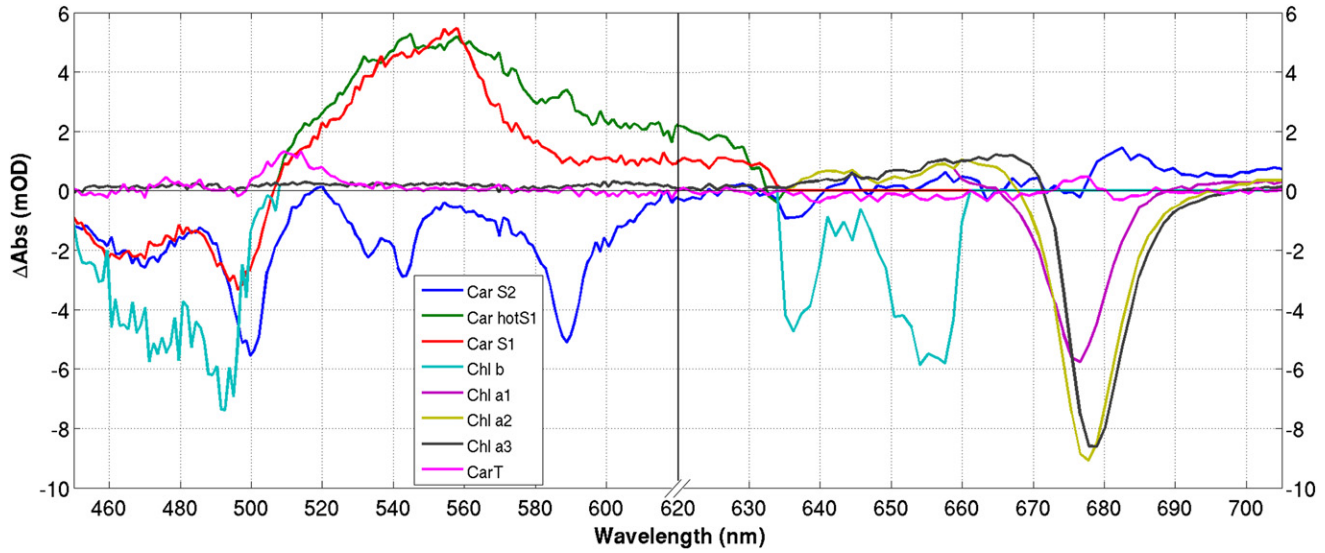

FIGURE 5 Target analysis results (SADS) of the pump-probe measurements on CP26 at 77 K after 506 nm excitation. Notice the change in scaling of the *x* axis at 620 nm.

was found for the Car hot S_1 state meaning that the 0.52 ps lifetimes in the second transition of the global analysis is the result of Car hot S_1 dynamics. The Car S_1 decay was fitted with a 14.7 ps lifetime very similar to CP26. The corresponding Car S_1 SADS shows a pronounced ESA peak at 559 nm. Between the four Chl components extracted in the Qy region, Chl a1 corresponds to the Chl species at 670 nm. This component decays in 3.5 ps, in perfect agreement with our previous study (45). To avoid artifacts in the SADS of Chl *b* originating from spectral and temporal overlap of different species, assumptions were made about the spectral shape of the SADS (see Materials and Methods). The last three SADS describe the decay of the Chl Qy excitation (in 8.3 ps and 2.7 ns) and the rise of the CarT state.

DISCUSSION

Spectrum of the carotenoid S_2 states

The first EADS of Fig. 2 or SADS1 of Fig. 5 (CP26) include bands at 533, 543 nm, and at 589 nm. Peaks in the same spectral region were found in solution at 77 K for Lut (ca. 530, 570 nm), Vio (ca. 520, 560 nm) (50) and for Neo at room temperature (540 and 575 nm) (51,52). The

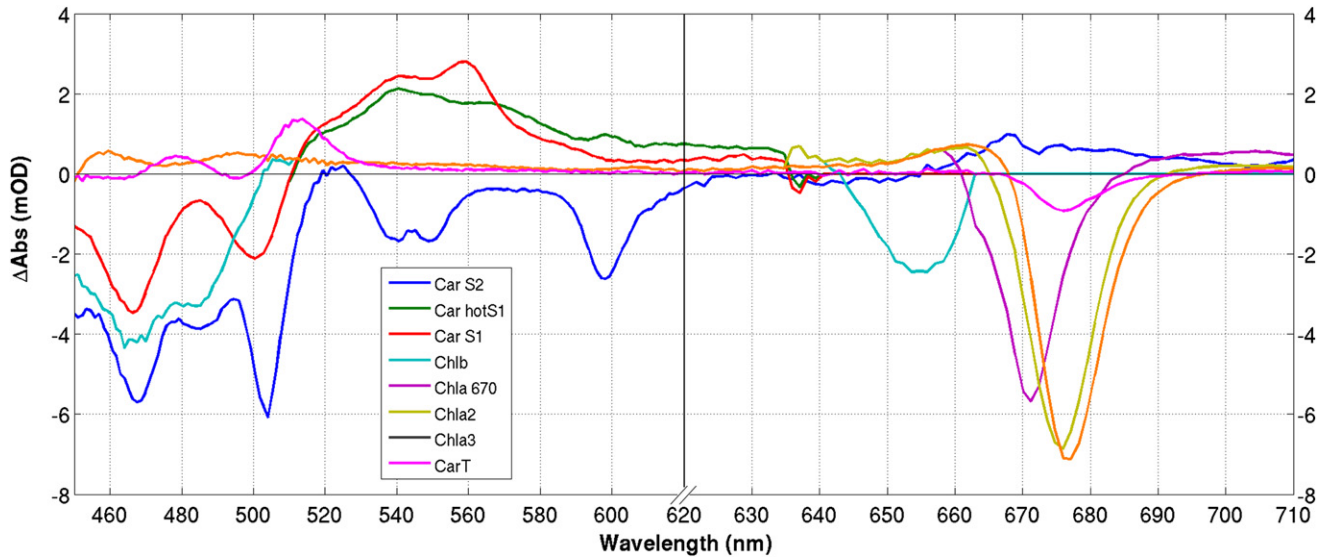

FIGURE 6 Target analysis results (SADS) of the pump-probe measurements on CP24 at 77 K after 506 nm excitation. Notice the change in scaling of the *x* axis at 620 nm.

EADS1 of CP24 shows peaks at 530, 542, and 588 nm after 506 nm excitation and at 518, 529, and 573 nm after 490 nm excitation (Figs. 3 and 4). The energy differences with the bleaching of the bands lie in three defined ranges: 1110–1340, 1500–1620, and 2975–3110 cm^{-1}, respectively. The bands in the first two ranges are similar to previously measured resonance stimulated Raman spectra of β-caroteine (53) corresponding to the Car $\nu 2$ and $\nu 1$ bands of resonance Raman (54). The bands between 2975 cm^{-1} and 3110 cm^{-1} are close to the stimulated Raman contribution of the solvent, which in standard resonance is centered around 3400 cm^{-1} for water and glycerol. Therefore, the observed bands are likely due to resonance stimulated Raman scattering of Cars and of the solvent.

Notably, these bands and the ESA above 628 nm present analogies with the SE bands at similar wavelengths shown in the 50 fs differential transmission spectra of Cerullo, Polli and co-workers (55,56). In those works however, these features were attributed to an ultrafast decaying S_x state mediating S_2 to S_1 conversion.

Transfer from the carotenoid S_2 states

In the first EADS of CP26 (Fig. 2) Chl *b* bleach is present at 637 and 651.5 nm. This can be due to direct excitation, but could also originate from ultrafast Car to Chl *b* transfer or strong Cars-Chl interactions. The presence of this Chl *b* bleaching makes it difficult to estimate if EET to Chls *b* occurs during the first transition, although in target analysis a 10% transfer from the Car S_2 to the Chl *b* compartments was found. This transfer, if true, possibly originates from the small amount of Neo directly excited, as it was shown that Neo in the N1 site of CP26 is located in proximity of Chls *b* (23).

In the Chl *a* Qy region of CP26, the Chl *a* increase indicates transfer to two Chl *a* populations at 674–675 and 678–679 nm. The bluer Chls *a* form at 674–675 nm is possibly the Chl *a*602-*a*603 cluster, which interacts with Lut-L2 (21). The redder form at 678–679 nm is close to the spectral position of the lowest energy state of CP26 (Chl *a*611-*a*612), which is located very close to Lut-L1 (38).

For CP24 excited at 506 nm, a clear transfer from the Car S_2 state to Chl *b*-650 nm is observed in the first transition, corresponding to 30% of the Car excitation. Another 25% is transferred to Chl *a* acceptors absorbing mainly at 670 nm. It has been proposed for CP24 that Lut-L1 is close to Chls *a*, whereas Vio-L2 is close to both Chls types (22). Thus, it is probable that the observed EET from S_2 to the Chls *b* originates mainly from excited Vio, indicating that the 490 nm excitation is partially selective for Vio.

Summarizing, transfer to Chls *a* occurs in CP26 to two Chl *a* populations: to the lowest energy states at 678–679 nm and to a Chl *a* form at 674–675 nm, which we identify with Chl *a*612 and Chl *a*603, respectively. In CP24 after 506 nm excitation the Chls *a* acceptors absorb at 670 nm, whereas a significant amount of excitation is transferred directly to Chls *b*.

The carotenoid S_1 states

In this study, we are able to separate the vibrationally hot S_1 states (47,48) from S_2 and S_1. Car S_1 spectra are an important reference for pump-probe studies on nonphotochemical quenching, since the NPQ research community is debating over an energy dissipation pathway involving the lower excited state of Lut (40,57) or excitonic Cars-Chls states (41). The shape of the S_1-Sn spectrum is thus important to be able to discriminate between the involvement of a pure S_1 state or of a mixing of the S_1 state with a charge transfer state.

Transfer from the carotenoid hot S_1

In both CP26 and CP24, the decay of the hot S_1 state takes place in parallel with EET from Chls *b* to Chls *a*. In CP26, the Chl *b* decay was fitted with a 0.73 ps lifetime (Fig. 7 *A*), a compromise between the two 0.21 and 1.5 ps lifetimes found after direct Qy excitation (45). During the second transition (Fig. 2) the Chl *a* bleaching doubles in area/amplitude, with a gain centered at 678–679 nm. The balance in decayed Chl *b*/gained Chl *a* areas reveals that the former is not sufficient to explain the Chl *a* increase. In fact, assuming a ratio of 0.65–0.7 between the extinction coefficients of Chl *b* and Chl *a* (58,59), we find a 24.9 Chl *b* decay and a 36.4 Chl *a* gain. This supports EET from the Car to the Chl *a* states. The possible donor is Lut-L1, as it is in contact with the Chls *a*610-*a*611-*a*612 at low energies.

In the same way, the balance in area in CP24 excited at 506 nm shows an additional transfer from hot S_1 to the Chls *a* (7.1 Chl *b* decay and a 14.0 Chl *a* gain).

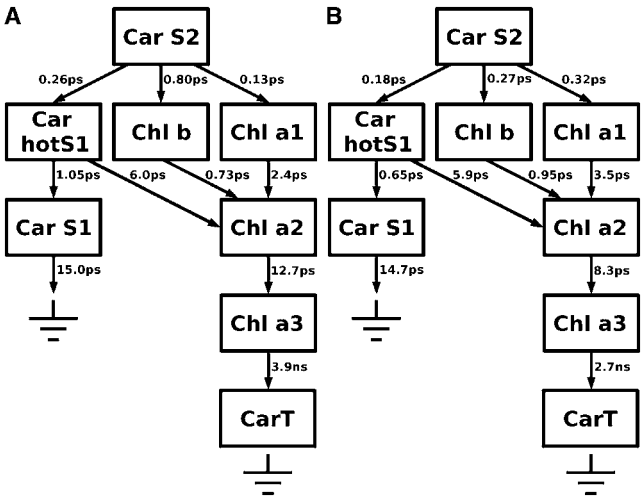

FIGURE 7 Compartmental scheme used in the target analysis and reciprocal of the rate constants expressed in ps for CP26 (*A*) and CP24 (*B*). See Materials and Methods for the spectral constraints used.

In CP24, the Chl *b* band decays in 0.95 ps (target analysis in Fig. 7 *B*), i.e., in a transition that is not captured by the global analysis. This transition is mainly due to the fast Chls *b* decay (lifetimes of 0.61 and 3.6 ps were found after Chl *b* excitation (45)), indicating that transfer from Cars involves mainly one of the two Chl *b* clusters. Transfer from the Chl *b* involves a Chl *a* population at 675 nm corresponding to the lowest energy states of CP24 Chl *a*611-*a*612 (45).

In conclusion, our findings suggest that in both complexes EET occurs from hot S_1.

The carotenoid S_1 states are not involved in energy transfer

In CP26, no significant change in Chl *a* Qy bleaching occurs during the Car S_1 decay and negligible Chl *b* signal is present (third and fourth EADS, Fig. 2). Hence, this gives no indications for Car S_1 to Chl transfer. Also in the CP24 data sets the fourth 20.5/24.0 ps transitions show a small decay of the Chl Qy band. This indicates that also in CP24 the transfer from Car S_1 states, if present, is negligible. The absence of transfer from Lut S_1 is confirmed by the fact that the S_1 lifetimes observed in both complexes upon 506 nm excitation are similar to the Lut S_1 lifetime in solution (19.7/15.6 ps at RT/77 K in pyridine/EPA solution (50)). Regarding Vio in the L2 site of CP24, we find no evidence for a slower ~30 ps component typical of Vio in solution (26.4/33.5 ps at RT/77 K (50)). However, upon excitation at 490 nm we observed a relatively longer S_1 lifetime than upon 506 nm excitation. This 19.8 ps S_1 decay (Fig. S5) might represent an intermediate value from the S_1 lifetimes of Lut and Vio, indicating possible photoselection of a larger amount of Vio-L2 at 490 nm. The fact that the decay is still relatively short as compared to solution can be due to the high transfer efficiency of Vio-L2 from the S_2 state leading to a small population of the Vio S_1 state, with the consequence that even upon 490 nm excitation the S_1 decay is dominated by Lut.

Lhc complexes compared

CP26 was shown to share several similarities with LHCII, in particular spectral properties, EET dynamics, structural and pigment organization (19,45,60). In LHCII (27) and Lhcb1 (A. Marin, unpublished results) however, the Chl *a* forms at low energies are flanked by excited Chls *a* forming a distinct shoulder ~7–10 nm off the peak. In LHCII, these Chls are populated directly from the carotenoid S_2 state and they decay in 7–8 ps ((27); A. Marin, unpublished results). This shoulder is not observed in the spectra of CP26 upon carotenoid excitation and it is also missing after excitation in the Qy region (45). As discussed previously (45), it is likely that the absence of this form originates from the functional disruption of the bottleneck states (Chls *a*604-*b*605) in CP26, which also suggests that Chl 604 in LHCII is involved in the Car to Chl EET.

In CP26, EET from the Cars is mainly directed to Chls *a* (60%) and involves the low-energy Chls (*a*611-*a*612) and Chls *a* at slightly higher energies (Chl *a*602-*a*603), which interact with Lut-L1 and Lut-L2, respectively. The small amount of transfer to the Chls *b* (maximum 10%) probably originates from Neo in the N1 site, which is the most blue-shifted xanthophyll associated with CP26—maximum at 488 nm—and is probably weakly excited at 506 nm.

CP24 is characterized by a distinct band at 670 nm decaying in 3–4 ps after Chl excitation (45), and in 3.3–3.6 ps after being populated by the Cars. The fact that Car S_2 states selectively populate this species and not Chls *a* at low energies is a unique behavior of CP24 between the Photosystem II antennas. The 670 nm species was assigned to Chl *a*602 and/or *a*603 on the helix B domain of the complex close to Vio-L2 (45). This means that in CP24 no strong interactions are present between Lut-L1 and the low-energy states, confirming that the domain formed by Lut-L1, Chls *a*611, and *a*612 has a different pigment organization as compared to the other Lhc complexes (38). The transfer to Chls *b* in 80 fs can be attributed to Vio-L2, because Lut-L1 was shown to have no Chls *b* at short distance (22).

We have found no indication for transfer from Lut S_1 in CP26, CP24, and Lhcb1 (A. Marin, unpublished results), which suggests the Lut S_1 energy levels is below the Chl *a*/*b* Qy states. The same result was found by Polívka et al. with Vio and Zea in solution (61) and in reconstituted LHCII (62). In CP29 transfer from S_1 was found from Vio (29), which has excited states at higher energies than Lut (63). From these considerations we imply that in most LHCs Lut S_1 state can potentially accept energy from Chls and act as quencher.

SUPPORTING MATERIAL

Five figures are available at http://www.biophysj.org/biophysj/supplemental/S0006-3495(11)00474-7.

Alessandro Marin is grateful to Fred Etoc for his collaboration during preliminary investigations, to Miroslav Kloz and Bruno Robert for useful discussions, and to John Kennis for organizing the access to the Multi-Pulse setup.

This work was supported by the Netherlands Organization for Scientific Research-Chemical Sciences through a TOP grant to R.v.G. and Earth and Life Science (ALW) through a Vidi grant to R.C.

REFERENCES

1. Loll, B., J. Kern, …, J. Biesiadka. 2005. Towards complete cofactor arrangement in the 3.0 Å resolution structure of photosystem II. *Nature.* 438:1040–1044.
2. Boekema, E. J., H. Van Roon, …, J. P. Dekker. 1999. Supramolecular organization of photosystem II and its light-harvesting antenna in partially solubilized photosystem II membranes. *Eur. J. Biochem.* 266:444–452.

3. Caffarri, S., R. Kouril, …, R. Croce. 2009. Functional architecture of higher plant photosystem II supercomplexes. *EMBO J.* 28:3052–3063.
4. Croce, R., and H. van Amerongen. 2011. Light-harvesting and structural organization of Photosystem II: from individual complexes to thylakoid membrane. *J. Photochem. Photobiol. B*. 10.1016/j.jphotobiol.2011.02.015.
5. Demmig-Adams, B., and W. W. I. I. I. Adams, 3rd. 2002. Antioxidants in photosynthesis and human nutrition. *Science.* 298:2149–2153.
6. Horton, P., A. V. Ruban, and R. G. Walters. 1996. Regulation of light harvesting in green plants. *Annu. Rev. Plant Physiol. Plant Mol. Biol.* 47:655–684.
7. Niyogi, K. K. 1999. Photoprotection revisited: genetic and molecular approaches. *Annu. Rev. Plant Physiol. Plant Mol. Biol.* 50:333–359.
8. Liu, Z., H. Yan, …, W. Chang. 2004. Crystal structure of spinach major light-harvesting complex at 2.72 Å resolution. *Nature.* 428:287–292.
9. Standfuss, J., A. C. Terwisscha van Scheltinga, …, W. Kühlbrandt. 2005. Mechanisms of photoprotection and nonphotochemical quenching in pea light-harvesting complex at 2.5 Å resolution. *EMBO J.* 24: 919–928.
10. Croce, R., S. Weiss, and R. Bassi. 1999. Carotenoid-binding sites of the major light-harvesting complex II of higher plants. *J. Biol. Chem.* 274:29613–29623.
11. Hobe, S., H. Niemeier, …, H. Paulsen. 2000. Carotenoid binding sites in LHCIIb. Relative affinities towards major xanthophylls of higher plants. *Eur. J. Biochem.* 267:616–624.
12. Caffarri, S., R. Croce, …, R. Bassi. 2001. The major antenna complex of photosystem II has a xanthophyll binding site not involved in light harvesting. *J. Biol. Chem.* 276:35924–35933.
13. Ruban, A. V., P. J. Lee, …, P. Horton. 1999. Determination of the stoichiometry and strength of binding of xanthophylls to the photosystem II light harvesting complexes. *J. Biol. Chem.* 274:10458–10465.
14. Pan, X., M. Li, …, W. Chang. 2011. Structural insights into energy regulation of light-harvesting complex CP29 from spinach. *Nat. Struct. Mol. Biol.* 18:309–315.
15. Plumley, F. G., and G. W. Schmidt. 1987. Reconstitution of chlorophyll *a/b* light-harvesting complexes: xanthophyll-dependent assembly and energy transfer. *Proc. Natl. Acad. Sci. USA.* 84:146–150.
16. Paulsen, H., U. Rümler, and W. Rüdiger. 1990. Reconstitution of pigment-containing complexes from light-harvesting chlorophyll *a/b*-binding protein overexpressed in *Escherichia coli*. *Planta.* 181:204–211.
17. Frank, H. A., J. A. Bautista, …, A. J. Young. 2000. Mechanism of nonphotochemical quenching in green plants: energies of the lowest excited singlet states of violaxanthin and zeaxanthin. *Biochemistry.* 39:2831–2837.
18. Gastaldelli, M., G. Canino, …, R. Bassi. 2003. Xanthophyll binding sites of the CP29 (Lhcb4) subunit of higher plant photosystem II investigated by domain swapping and mutation analysis. *J. Biol. Chem.* 278:19190–19198.
19. Croce, R., G. Canino, …, R. Bassi. 2002. Chromophore organization in the higher-plant photosystem II antenna protein CP26. *Biochemistry.* 41:7334–7343.
20. Bassi, R., R. Croce, …, D. Sandonà. 1999. Mutational analysis of a higher plant antenna protein provides identification of chromophores bound into multiple sites. *Proc. Natl. Acad. Sci. USA.* 96:10056–10061.
21. Ballottari, M., M. Mozzo, …, R. Bassi. 2009. Occupancy and functional architecture of the pigment binding sites of photosystem II antenna complex Lhcb5. *J. Biol. Chem.* 284:8103–8113.
22. Passarini, F., E. Wientjes, …, R. Croce. 2009. Molecular basis of light harvesting and photoprotection in CP24: unique features of the most recent antenna complex. *J. Biol. Chem.* 284:29536–29546.
23. Caffarri, S., F. Passarini, …, R. Croce. 2007. A specific binding site for neoxanthin in the monomeric antenna proteins CP26 and CP29 of Photosystem II. *FEBS Lett.* 581:4704–4710.
24. Polívka, T., and V. Sundström. 2004. Ultrafast dynamics of carotenoid excited states – From solution to natural and artificial systems. *Chem. Rev.* 104:2021–2071.
25. Peterman, E. J., C. C. Gradinaru, …, H. van Amerongen. 1997. Xanthophylls in light-harvesting complex II of higher plants: light harvesting and triplet quenching. *Biochemistry.* 36:12208–12215.
26. Connelly, J. P., M. G. Müller, …, A. R. Holzwarth. 1997. Femtosecond transient absorption study of carotenoid to chlorophyll energy transfer in the light-harvesting complex II of photosystem II. *Biochemistry.* 36:281–287.
27. Gradinaru, C., I. H. M. van Stokkum, …, H. van Amerongen. 2000. Identifying the pathways of energy transfer between carotenoids and chlorophylls in LHCII and CP29. A multicolor pump-probe study. *J. Phys. Chem.* 104:9330–9342.
28. Croce, R., M. G. Müller, …, A. R. Holzwarth. 2001. Carotenoid-to-chlorophyll energy transfer in recombinant major light-harvesting complex (LHCII) of higher plants. I. Femtosecond transient absorption measurements. *Biophys. J.* 80:901–915.
29. Croce, R., M. G. Müller, …, A. R. Holzwarth. 2003. Energy transfer pathways in the minor antenna complex CP29 of photosystem II: a femtosecond study of carotenoid to chlorophyll transfer on mutant and WT complexes. *Biophys. J.* 84:2517–2532.
30. Gradinaru, C. C., R. van Grondelle, and H. van Amerongen. 2003. Selective interaction between xanthophylls and chlorophylls in LHCII probed by femtosecond transient absorption spectroscopy. *J. Phys. Chem. B.* 107:3938–3943.
31. Barzda, V., E. J. Peterman, …, H. van Amerongen. 1998. The influence of aggregation on triplet formation in light-harvesting chlorophyll *a/b* pigment-protein complex II of green plants. *Biochemistry.* 37:546–551.
32. Mozzo, M., L. Dall'Osto, …, R. Croce. 2008. Photoprotection in the antenna complexes of photosystem II: role of individual xanthophylls in chlorophyll triplet quenching. *J. Biol. Chem.* 283:6184–6192.
33. Peterman, E. J., F. M. Dukker, …, H. van Amerongen. 1995. Chlorophyll *a* and carotenoid triplet states in light-harvesting complex II of higher plants. *Biophys. J.* 69:2670–2678.
34. Carbonera, D. 2009. Optically detected magnetic resonance (ODMR) of photoexcited triplet states. *Photosynth. Res.* 102:403–414.
35. Lampoura, S. S., V. Barzda, …, H. van Amerongen. 2002. Aggregation of LHCII leads to a redistribution of the triplets over the central xanthophylls in LHCII. *Biochemistry.* 41:9139–9144.
36. Naqvi, K. R., T. B. Melø, …, G. Garab. 1997. Quenching of chlorophyll *a* singlets and triplets by carotenoids in light-harvesting complex of photosystem II: comparison of aggregates with trimers. *Spectrochim. Acta A.* 53:2659–2667.
37. Van der Vos, R., E. M. Franken, and A. J. Hoff. 1994. ADMR study of the effect of oligomerisation on the carotenoid triplets and on triplet-triplet transfer in light harvesting complex II (LHC II) of spinach. *Biochim. Biophys. Acta.* 1188:243–250.
38. Mozzo, M., F. Passarini, …, R. Croce. 2008. Photoprotection in higher plants: the putative quenching site is conserved in all outer light-harvesting complexes of Photosystem II. *Biochim. Biophys. Acta.* 1777:1263–1267.
39. Georgakopoulou, S., G. van der Zwan, …, R. Croce. 2007. Understanding the changes in the circular dichroism of light harvesting complex II upon varying its pigment composition and organization. *Biochemistry.* 46:4745–4754.
40. Ruban, A. V., R. Berera, …, R. van Grondelle. 2007. Identification of a mechanism of photoprotective energy dissipation in higher plants. *Nature.* 450:575–578.
41. Bode, S., C. C. Quentmeier, …, P. J. Walla. 2009. On the regulation of photosynthesis by excitonic interactions between carotenoids and chlorophylls. *Proc. Natl. Acad. Sci. USA.* 106:12311–12316.
42. Ahn, T. K., T. J. Avenson, …, G. R. Fleming. 2008. Architecture of a charge-transfer state regulating light harvesting in a plant antenna protein. *Science.* 320:794–797.

43. Li, Z., T. K. Ahn, …, K. K. Niyogi. 2009. Lutein accumulation in the absence of zeaxanthin restores nonphotochemical quenching in the *Arabidopsis thaliana npq1* mutant. *Plant Cell.* 21:1798–1812.

44. van Amerongen, H., and R. van Grondelle. 2000. Understanding the energy transfer function of LHCII, the major light-harvesting complex of green plants. *J. Phys. Chem. B.* 105:604–617.

45. Marin, A., F. Passarini, …, R. van Grondelle. 2010. Energy transfer pathways in the CP24 and CP26 antenna complexes of higher plant photosystem II: a comparative study. *Biophys. J.* 99:4056–4065.

46. van Stokkum, I. H. M., D. S. Larsen, and R. van Grondelle. 2004. Global and target analysis of time-resolved spectra. *Biochim. Biophys. Acta.* 1657:82–104.

47. de Weerd, F. L., I. H. M. van Stokkum, …, R. van Grondelle. 2002. Pathways for energy transfer in the core light-harvesting complexes CP43 and CP47 of photosystem II. *Biophys. J.* 82:1586–1597.

48. Billsten, H. H., D. Zigmantas, …, T. Polívka. 2002. Dynamics of vibrational relaxation in the S1 state of carotenoids having 11 conjugated C=C bonds. *Chem. Phys. Lett.* 355:465–470.

49. Niedzwiedzki, D. M., J. O. Sullivan, …, H. A. Frank. 2006. Femtosecond time-resolved transient absorption spectroscopy of xanthophylls. *J. Phys. Chem. B.* 110:22872–22885.

50. Cong, H., D. M. Niedzwiedzki, …, H. A. Frank. 2008. Ultrafast time-resolved spectroscopy of xanthophylls at low temperature. *J. Phys. Chem. B.* 112:3558–3567.

51. Josue, J. S., and H. A. Frank. 2002. Direct determination of the S1 excited-state energies of xanthophylls by low-temperature fluorescence spectroscopy. *J. Phys. Chem. A.* 106:4815–4824.

52. Mimuro, M., U. Nagashima, …, T. Katoh. 1992. Molecular structure and optical properties of carotenoids for the in vivo energy transfer function in the algal photosynthetic pigment system. *Biochim. Biophys. Acta.* 1098:271–274.

53. Kukura, P., D. W. McCamant, …, R. A. Mathies. 2003. Vibrational structure of the S(2) (1B(u)) excited state of diphenyloctatetraene observed by femtosecond stimulated Raman spectroscopy. *Chem. Phys. Lett.* 382:81–86.

54. Robert, B. 2009. Resonance Raman spectroscopy. *Photosynth. Res.* 101:147–155.

55. Cerullo, G., D. Polli, …, R. J. Cogdell. 2002. Photosynthetic light harvesting by carotenoids: detection of an intermediate excited state. *Science.* 298:2395–2398.

56. Polli, D., G. Cerullo, …, R. J. Cogdell. 2006. Carotenoid-bacteriochlorophyll energy transfer in LH2 complexes studied with 10-fs time resolution. *Biophys. J.* 90:2486–2497.

57. Müller, M. G., P. Lambrev, …, A. R. Holzwarth. 2010. Singlet energy dissipation in the photosystem II light-harvesting complex does not involve energy transfer to carotenoids. *ChemPhysChem.* 11:1289–1296.

58. Lichtentaler, H. K. 1987. Chlorophylls and carotenoids: pigments of photosynthetic biomembranes. *In* Plant Cell Membranes. L. Packer, editor. Academic Press, San Diego, CA. 350–382.

59. Davies, B. H. 1976. Carotenoids. *In* Chemistry and Biochemistry of Plant Pigments, Vol 2. T. W. Goodwin, editor. Academic Press, London. 38–168.

60. Frank, H. A., S. K. Das, …, R. Bassi. 2001. Photochemical behavior of xanthophylls in the recombinant photosystem II antenna complex, CP26. *Biochemistry.* 40:1220–1225.

61. Polívka, T., J. L. Herek, …, V. Sundström. 1999. Direct observation of the (forbidden) S1 state in carotenoids. *Proc. Natl. Acad. Sci. USA.* 96:4914–4917.

62. Polívka, T., D. Zigmantas, …, R. Bassi. 2002. Carotenoid S(1) state in a recombinant light-harvesting complex of Photosystem II. *Biochemistry.* 41:439–450.

63. Polívka, T., and H. A. Frank. 2010. Molecular factors controlling photosynthetic light harvesting by carotenoids. *Acc. Chem. Res.* 43: 1125–1134.